

Light emission from tunnel junctions: The role of multiple scattering of surface polaritons

K. Arya* and R. Zeyher

Max-Planck-Institut für Festkörperforschung, D-7000 Stuttgart 80, Federal Republic of Germany

(Received 22 April 1983)

Calculations of light emission intensities from Al-Al₂O₃-metal tunnel junctions with randomly rough metal (Ag or Au) surface are presented. Multiple scattering of surface polaritons is taken into account by solving a previously derived Bethe-Salpeter equation for the averaged two-photon Green's function. The calculated intensities and the angular dependence of the emitted *s*- and *p*-polarized radiation are in good agreement with the experiments. We also point out that our nonperturbative treatment of roughness is essential for this good agreement.

I. INTRODUCTION

In 1976 Lambe and McCarthy¹ reported a new method for the generation of light using a tunnel junction. A metal-oxide-metal (MOM) tunnel junction consists of two metal films separated by a thin oxide layer. One metal is usually Al or Mg and the other is Ag or Au. The surface of the latter is usually rough. When a dc voltage is applied the junction starts emitting light. Owing to the applied voltage, electrons tunnel through the oxide layer and excite the surface polariton modes associated with the MOM layered structure. These local modes are nonradiative. In the presence of a rough surface they can, however, decay into radiative modes and thus cause the emission of light.

Since the first observation of Lambe and McCarthy there has been increased interest both experimentally²⁻⁹ and theoretically¹⁰⁻¹⁶ in the microscopic understanding of this phenomenon and in giving quantitative results for the emitted intensity. The problem can be treated in two steps:

- (i) The calculation of the coupling of tunneling electrons and surface polaritons (SP).
- (ii) The calculation of the efficiency of the decay of these excited polaritons into radiative photons due to the roughness.

The first step has been discussed by Davis¹⁰ for two semi-infinite metals separated by an oxide barrier and also in Refs. 11 and 16. The second step has been treated in a series of papers by Laks and Mills¹¹⁻¹³ and by Scalapino and co-workers.^{15,16} The former authors¹¹ consider a randomly rough Ag (or Au) surface, and the emitted intensity is calculated by taking a statistical average over all physical equivalent surface profiles. The distribution of these profiles is assumed to be Gaussian and specified by a root-mean-square roughness amplitude δ and a transverse correlation length a . Using a Green's function technique, they derive an expression for the emitted intensity which involves the calculations of the averaged two-photon Green's function. Assuming roughness as a weak perturbation over a flat surface, the intensity of the emitted light is calculated using first-order perturbation theory. Scalapino *et al.*¹⁶ consider light emission from a spherical par-

ticle put on top of an oxide layer formed on a flat metallic surface. They calculate the emitted intensity by directly solving the Maxwell equations neglecting retardation effects.

Both of these approaches do explain some of the experimental results. However, there remain serious disagreements. For instance, (a) the calculated emission intensities of Laks and Mills,¹¹ for experimental values of the roughness parameters ($\delta \sim 50$ Å, $a \sim 300-400$ Å), are much too small compared with the experiments. The observed intensities can only be obtained for unrealistic small values of a ($a < 100$ Å). The model of Scalapino *et al.*¹⁶ predicts the correct magnitude for the emitted light intensity. (b) In regard to the polarization and angular distribution of the light, neither calculation is able to explain the experimental results. For instance, experiments of Adams, Wyss, and Hansma⁴ find both *s*- and *p*-polarized components present in the emission. The *s*-polarized light has maximum intensity along the normal to the metal surface and then falls smoothly to zero in a direction along the surface. The *p*-polarized light, whose intensity is equal to that of *s*-polarized light along the normal, shows a lobe structure in a direction that makes roughly an angle of 50° with the normal. Laks and Mills find that the emitted light has both *s*- and *p*-polarized components. The angular distribution of *s* photons is in agreement with the experiments, however, the *p*-polarized light does not show any maxima off the normal. The calculations of Scalapino *et al.*¹⁶ do not give any *s*-polarized light. The *p*-polarized light shows a lobe structure around 50° with the normal, however, its intensity becomes zero along the normal in disagreement with the experiments.

In this paper we consider a tunnel junction with a randomly rough metal surface. We use the same formula for the calculations of the intensity of the emitted light as used by Laks and Mills.¹¹ The difference between our calculations and theirs lies in the different approximations for the averaged two-photon propagator. In an earlier paper,¹⁷ we have shown that this quantity satisfies a Bethe-Salpeter equation whose kernel is given by a functional derivative of the self-energy of the averaged one-photon propagator. If terms proportional to δ^2 alone are retained in the self-energy, then the corresponding integral equation represents the ladder summation that includes multiple scattering of the surface polaritons at the rough sur-

face. Within this approximation we have solved the Bethe-Salpeter equation exactly for the averaged two-photon Green's function. The results of Laks and Mills correspond to a lowest-order perturbation treatment to the solution of this equation. We, however, find that for the experimental values of the roughness parameters δ and a and, in particular, for the values used in Ref. 11, it is necessary to use our nonperturbative treatment for the roughness. The multiple scattering of SP increases the effective interaction of SP with the roughness and thus leads to large emission intensities in agreement with experiments. We include in the calculations both the slow as well as the fast SP. The contribution due to fast SP, which has been neglected in Ref. 11, is found to be particularly important for large values of a .

In Sec. II A, we introduce our notations and the expression for the intensity of emitted light in terms of an averaged two-photon Green's function. Section II B contains the main part of this paper. First we derive a Dyson equation for the averaged one-photon propagator and give explicit expression for the self-energy to the lowest order δ . The corresponding Bethe-Salpeter equation representing the ladder summation is then solved in order to calculate emission intensities. The calculated intensities for various values of roughness parameters δ and a are given in Sec. III.

II. THEORETICAL FRAMEWORK

A. Intensity of emitted light

Let us consider a semi-infinite metal substrate with dielectric constant $\epsilon_3(\omega)$. The substrate is overlaid with an oxide layer of thickness d and this by a metal film of nominal thickness L (Fig. 1). The dielectric constant of the oxide layer and of the metal film are assumed to be $\epsilon_2(\omega)$ and $\epsilon_1(\omega)$, respectively. In general $\epsilon_1(\omega)$, $\epsilon_2(\omega)$, and $\epsilon_3(\omega)$ can be complex. The z axis of the coordinate system is normal to the surface of the substrate, and its surface coincides with x - y plane. Finally, the surface of the metal film is roughened. The location of a point on the surface

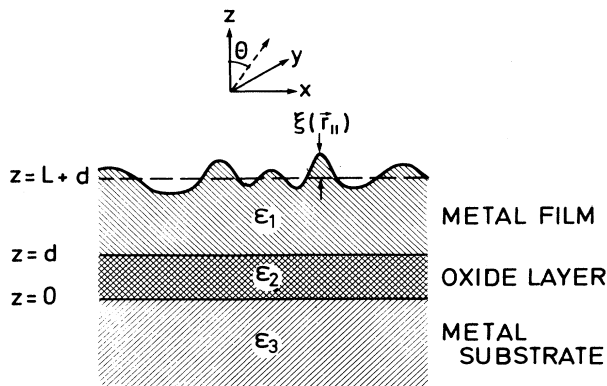


FIG. 1. Geometry of the considered tunnel junction. $\epsilon_i(\omega)$ are the corresponding dielectric functions and $\zeta(\vec{r}_{\parallel})$ the profile function for the rough surface of the metal film.

is defined by the relation $z=L+d+\zeta(\vec{r}_{\parallel})$ with $\vec{r}_{\parallel}=x\hat{x}+y\hat{y}$. The function $\zeta(\vec{r}_{\parallel})$ thus describes the roughness profile on the outer surface.

Let a dc voltage V be applied across the junction and $\vec{J}(\vec{r},t)$ be the fluctuating current density due to the tunneling electrons in the junction. The electric field $\vec{E}(\vec{r},\omega)$ due to this current can be written as

$$E_i(\vec{r},\omega) = \frac{i\omega}{c^2} \sum_j \int d^3r' \hat{d}_{ij}(\vec{r},\vec{r}',\omega) J_j(\vec{r}',\omega), \quad (1)$$

where

$$J_j(\vec{r},t) = \int_{-\infty}^{\infty} \frac{d\omega}{2\pi} J_j(\vec{r},\omega) e^{-i\omega t}. \quad (2)$$

$\hat{d}_{ij}(\vec{r},\vec{r}',\omega)$ is the photon Green's function which satisfies the following Maxwell's equation:

$$-\vec{\nabla} \times \vec{\nabla} \times \vec{\hat{d}}(\vec{r},\vec{r}',\omega) + (\omega^2/c^2)\epsilon(\vec{r},\omega)\vec{\hat{d}}(\vec{r},\vec{r}',\omega) = 4\pi\delta(\vec{r}-\vec{r}')\vec{I}, \quad (3)$$

where

$$\begin{aligned} \epsilon(\vec{r},\omega) = & \epsilon_3(\omega)\Theta(-z) + \epsilon_2(\omega)[\Theta(d-z) - \Theta(-z)] \\ & + \epsilon_1(\omega)[\Theta(L+d+\zeta(\vec{r}_{\parallel})-z) - \Theta(d-z)] \\ & + \Theta(z-L-d-\zeta(\vec{r}_{\parallel})) \end{aligned} \quad (4)$$

is the dielectric function of the layered structure (Fig. 1). In the solution of Eq. (3), for fixed \vec{r}' the outgoing wave boundary condition is used when $|\vec{r}| \rightarrow \infty$ in the vacuum. \hat{d}_{ij} goes to zero when $|\vec{r}| \rightarrow \infty$ into the substrate. We define Fourier transformations with respect to the coordinates parallel to the surface as follows:

$$\begin{aligned} \hat{d}_{ij}(\vec{r},\vec{r}',\omega) = & \int \frac{d^2k_{\parallel}}{(2\pi)^2} \int \frac{d^2k'_{\parallel}}{(2\pi)^2} e^{i\vec{k}_{\parallel}\cdot\vec{r}_{\parallel} + i\vec{k}'_{\parallel}\cdot\vec{r}'_{\parallel}} \\ & \times \hat{d}_{ij}(\vec{k}_{\parallel},\vec{k}'_{\parallel},\omega | z,z'). \end{aligned} \quad (5)$$

With the use of the outgoing boundary condition on \hat{d}_{ij} it can be shown that for $z \rightarrow \infty$ in the vacuum, one can write¹¹

$$\hat{d}_{ij}(\vec{k}_{\parallel},\vec{k}'_{\parallel},\omega | z,z') = e^{ik_0 z} \gamma_{ij}(\vec{k}_{\parallel},\vec{k}'_{\parallel},\omega | z'), \quad (6)$$

where

$$k_0 = \left[\frac{(\omega + i\eta)^2}{c^2} - k_{\parallel}^2 \right]^{1/2}. \quad (7)$$

In Eq. (7), η is positive infinitesimal and the square root is chosen with $\text{Im}(k_0) > 0$ always.

Knowing $\hat{d}_{ij}(\vec{r},\vec{r}',\omega)$ and hence $E_i(\vec{r},\omega)$ from Eq. (1) one can calculate the energy flux ($d^3W/d\Omega d\omega dt$), i.e., the energy radiated per unit time, per unit solid angle $d\Omega$, and per unit frequency $d\omega$. This has been discussed in detail in Ref. 11, and here we quote that result:

$$\frac{d^3W}{d\Omega d\omega dt} = \frac{\delta^4 \cos^2 \theta}{32\pi^3 c^5} \int d^2Q_{||} \int dz' \int dz'' \sum_{\mu, \lambda, \lambda'} \gamma_{\mu\lambda}(\vec{k}_{||}, \vec{Q}_{||}, \omega | z') \gamma_{\mu\lambda'}^*(\vec{k}_{||}, \vec{Q}_{||}, \omega | z'') \mathcal{F}_{\lambda\lambda'}(\vec{Q}_{||}, \omega | z', z''), \quad (8)$$

where $|\vec{k}_{||}| = (\omega/c)\sin\theta$, $k_0 = (\omega/c)\cos\theta$, and Θ gives the direction of the energy flux with respect to the z axis. $\mathcal{F}_{\lambda\lambda'}(\vec{Q}_{||}, \omega | z', z'')$ is a correlation function that is related to the frequency spectrum and spatial correlation of the tunnel-current fluctuations. An expression for $\mathcal{F}_{\lambda\lambda'}$ was derived by Rendell and Scalapino¹⁶ using the method of the tunneling Hamiltonian. Laks and Mills¹¹ included spatial decay of current correlations in the exponential form, and we use their expression. As discussed in Ref. 11 only $\mathcal{F}_{zz}(\vec{Q}_{||}, \omega | z', z'')$ is taken to be nonzero and a phenomenological form for this is

$$\mathcal{F}_{zz}(\vec{Q}_{||}, \omega | z, z') = \frac{eI(1 - \hbar\omega/eV)}{2\pi^2} \frac{\Delta(z, z')}{(1 + Q_{||}^2 \xi_0^2)^{3/2}}, \quad (9)$$

where I is the static current flowing in the junction, ξ_0 is a correlation parameter, and $\Delta(z, z')$ is taken to be unity. Equation (8) is written for a given surface profile of the rough metal surface. For any physical quantity to be compared with the experimental results, one must take the statistical average over all different surface profile functions. Furthermore, for comparison with the experiments, it is convenient to define the following dimensionless quantity:

$$\frac{dQ(\omega)}{d\Omega} = \frac{e^2 V}{\hbar^2 \omega I} \frac{d^3W}{d\Omega d\omega dt}. \quad (10)$$

Physically the integral $\int_0^{\omega_c} d\omega (\omega_c)^{-1} dQ/d\Omega$, where $\omega_c = eV/\hbar$ is the upper cutoff frequency, gives the probability per unit solid angle that one electron that has tunneled through the oxide barrier emits a photon in a given direction. Thus from Eqs. (8)–(10), we have

$$\frac{dQ(\omega)}{d\Omega} = \frac{e^2}{\hbar c} \left[\frac{eV}{\hbar\omega} - 1 \right] \frac{\omega^4 \cos^2 \theta}{16\pi^3 c^4} \int \frac{d^2Q_{||}}{(2\pi)^2} \int dz' \int dz'' \sum_{\mu} \langle \gamma_{\mu z}(\vec{k}_{||}, \vec{Q}_{||}, \omega | z') \gamma_{\mu z}^*(\vec{k}_{||}, \vec{Q}_{||}, \omega | z'') \rangle \frac{1}{(1 + Q_{||}^2 \xi_0^2)^{3/2}}, \quad (11)$$

where $\langle \dots \rangle$ denotes the statistical average over the ensemble of all profile functions. The problem is thus reduced to the calculation of the averaged two-photon Green's function, i.e.,

$$\langle \hat{d}_{ij}(\vec{k}_{||}, \vec{k}'_{||}, \omega | z, z') \hat{d}_{kl}^*(\vec{k}_{||}, \vec{k}'_{||}, \omega | z_1, z'_1) \rangle$$

Note \hat{d}_{ij} is related to γ_{ij} through an exponential factor [Eq. (6)]. A general, self-consistent method based on the functional derivative approach of Baym and Kadanoff^{18,19} to calculate this quantity has been given in Ref. 17. In the following section we specify the results of this general treatment to our case.

B. Averaged photon propagators

We split the dielectric function $\epsilon(\vec{r}, \omega)$ in Eq. (4) into two parts,

$$\epsilon(\vec{r}, \omega) = \epsilon^{(0)}(z, \omega) + [\epsilon_1(\omega) - 1]V(\vec{r}, \omega), \quad (12)$$

$$V(\vec{r}, \omega) = [\Theta(L + d + \zeta(\vec{r}_{||}) - z) - \Theta(L + d - z)]. \quad (13)$$

Here $\epsilon^{(0)}(z, \omega)$ is the dielectric function for the three-layer structure with smooth surfaces, and the second term in Eq. (12) gives the change in ϵ due to roughness. Let $d_{ij}^{(0)}(\vec{r}, \vec{r}', \omega)$ be the Green's function for the structure with a perfectly smooth surface, i.e., a solution of Eq. (3) with $\epsilon(\vec{r}, \omega)$ replaced by $\epsilon^{(0)}(z, \omega)$; then Eq. (3) can be converted into an integral equation

$$\hat{d}_{ij}(\vec{r}, \vec{r}', \omega) = d_{ij}^{(0)}(\vec{r}, \vec{r}', \omega) - \Lambda \sum_k \int d^3r'' d_{ik}^{(0)}(\vec{r}, \vec{r}'', \omega) V(\vec{r}'', \omega) \hat{d}_{kj}(\vec{r}'', \vec{r}', \omega), \quad (14)$$

$$\Lambda = (\omega^2/4\pi c^2)[\epsilon_1(\omega) - 1]. \quad (15)$$

Substituting Eq. (13) into Eq. (14), we have

$$\hat{d}_{ij}(\vec{r}, \vec{r}', \omega) = d_{ij}^{(0)}(\vec{r}, \vec{r}', \omega) - \Lambda \sum_k \int_{L+d}^{L+d+\zeta(\vec{r}_{||})} d^2r'' dz'' d_{ik}^{(0)}(\vec{r}, \vec{r}'', \omega) \hat{d}_{kj}(\vec{r}'', \vec{r}', \omega). \quad (16)$$

To perform the z'' integration, we take the limit $\zeta(\vec{r}_{||}) \rightarrow 0$, assuming the field varies smoothly close to the metal surface. As discussed in Ref. 11, one should be careful in taking this limit, as $d_{ik}^{(0)}(\vec{r}, \vec{r}'', \omega)$ has a jump discontinuity across the surface $z'' = L + d$ for the index k to be z . Following Ref. 11, we have

$$\hat{d}_{ij}(\vec{r}, \vec{r}', \omega) = d_{ij}^{(0)}(\vec{r}, \vec{r}', \omega) + \Lambda \sum_k \int d^2r'' [d_{ik}^{(0)}(\vec{r}_{||}, z; \vec{r}'', (L+d)+; \omega) \zeta(\vec{r}'') \hat{d}_{kj}(\vec{r}'', (L+d)-; \vec{r}'', z'; \omega)], \quad (17)$$

where $(L+d)\pm$ means slightly outside and inside the surface $z=L+d$, respectively. With the use of the Fourier transformations

$$d_{ij}^{(0)}(\vec{r}, \vec{r}', \omega) = \int \frac{d^2 k_{\parallel}}{(2\pi)^2} e^{i\vec{k}_{\parallel} \cdot (\vec{r}_{\parallel} - \vec{r}'_{\parallel})} d_{ij}^{(0)}(\vec{k}_{\parallel}, \omega | z, z'), \quad (18)$$

$$\xi(\vec{r}_{\parallel}) = \int \frac{d^2 k_{\parallel}}{(2\pi)^2} e^{i\vec{k}_{\parallel} \cdot \vec{r}_{\parallel}} \xi(\vec{k}_{\parallel}), \quad (19)$$

Eq. (17) can be written as

$$\begin{aligned} \hat{d}_{ij}(\vec{k}_{\parallel}, \vec{k}'_{\parallel}, \omega | z, z') &= (2\pi)^2 \delta(\vec{k}_{\parallel} + \vec{k}'_{\parallel}) d_{ij}^{(0)}(\vec{k}_{\parallel}, \omega | z, z') \\ &+ \Lambda \sum_k d_{ik}^{(0)}(\vec{k}_{\parallel}, \omega | z, (L+d)+) \int \frac{d^2 k''_{\parallel}}{(2\pi)^2} \xi(|\vec{k}_{\parallel} - \vec{k}''_{\parallel}|) \hat{d}_{kj}(\vec{k}''_{\parallel}, \vec{k}'_{\parallel}, \omega | (L+d)-, z'). \end{aligned} \quad (20)$$

Equation (20) is for one surface profile function. The averaged Green's function can be obtained by taking the statistical average over a distribution of these profiles, which we here assume to be Gaussian. The averaging is defined as

$$\langle \xi(\vec{k}_{\parallel}) \rangle = 0, \quad (21)$$

$$\langle \xi(\vec{k}_{\parallel}) \xi(\vec{k}'_{\parallel}) \rangle = (2\pi)^2 \delta(\vec{k}_{\parallel} + \vec{k}'_{\parallel}) \delta^2 g(|\vec{k}_{\parallel}|), \quad (22)$$

$$g(|\vec{k}_{\parallel}|) = \pi a^2 \exp(-k_{\parallel}^2 a^2 / 4), \quad (23)$$

where δ and a denote the root-mean-square roughness amplitude and transverse correlation length, respectively. With the use of Eqs. (21)–(23) in Eq. (20), the averaged one-photon Green's function

$$\langle \hat{d}_{ij}(\vec{k}_{\parallel}, \vec{k}'_{\parallel}, \omega | z, z') \rangle = (2\pi)^2 \delta(\vec{k}_{\parallel} + \vec{k}'_{\parallel}) d_{ij}(\vec{k}_{\parallel}, \omega | z, z') \quad (24)$$

can be expressed in terms of a Dyson equation^{20,21}

$$\begin{aligned} d_{ij}(\vec{k}_{\parallel}, \omega | z, z') &= d_{ij}^{(0)}(\vec{k}_{\parallel}, \omega | z, z') \\ &+ \sum_{k, k'} d_{ik}^{(0)}(\vec{k}_{\parallel}, \omega | z, (L+d)+) \Sigma_{kk'}(\vec{k}_{\parallel}, \omega | (L+d)-, (L+d)+) d_{kj}(\vec{k}_{\parallel}, \omega | (L+d)-, z'). \end{aligned} \quad (25)$$

The self-energy Σ_{ij} in comparison with Eq. (20) can be written as

$$\begin{aligned} \sum_k \Sigma_{ik}(\vec{k}_{\parallel}, \omega | (L+d)-, (L+d)+) d_{kj}(\vec{k}_{\parallel}, \omega | (L+d)-, z') \\ = \Lambda \int \frac{d^2 k'_{\parallel}}{(2\pi)^2} \int \frac{d^2 k''_{\parallel}}{(2\pi)^2} \langle \xi(\vec{k}_{\parallel} - \vec{k}''_{\parallel}) \hat{d}_{ij}(\vec{k}''_{\parallel}, \vec{k}'_{\parallel}, \omega | (L+d)-, z') \rangle. \end{aligned} \quad (26)$$

Equation (26) can be used to generate an expression of Σ in powers of d and g . The lowest-order term in δ is

$$\Sigma_{ij}(\vec{k}_{\parallel}, \omega | (L+d)-, (L+d)+) = \delta^2 \Lambda^2 \int \frac{d^2 k'_{\parallel}}{(2\pi)^2} g(|\vec{k}_{\parallel} - \vec{k}'_{\parallel}|) d_{ij}(\vec{k}'_{\parallel}, \omega | (L+d)-, (L+d)+). \quad (27)$$

Figure 2(a) illustrates the Dyson equation (25) for the averaged one-photon Green's function where the thin line denotes $d_{ij}^{(0)}$ and the thick line d_{ij} . Figure 2(b) shows the first two terms in the self-energy. The dashed line stands for the interaction term $\delta^2 \Lambda^2 g(|\vec{k}_{\parallel} - \vec{k}'_{\parallel}|)$.

The averaged two-photon Green's function can be written as

$$\langle \hat{d}_{ij}(\vec{k}_{\parallel}, \vec{k}'_{\parallel}, \omega | z_1, z_2) \hat{d}_{kl}^*(\vec{k}_{\parallel}, \vec{k}''_{\parallel}, \omega | z'_1, z'_2) \rangle = (2\pi)^2 \delta(\vec{k}_{\parallel} - \vec{k}''_{\parallel}) L_{ijkl}(\vec{k}_{\parallel}, \vec{k}'_{\parallel}, \omega | z_1, z'_1, z_2, z'_2). \quad (28)$$

In Ref. 17 it was shown that

$$L_{ijkl}(\vec{k}_{\parallel}, \vec{k}'_{\parallel}, \omega | (L+d)-, (L+d)-, (L+d)+, (L+d)+) \equiv L_{ijkl}(\vec{k}_{\parallel}, \vec{k}'_{\parallel}, \omega)$$

satisfies a Bethe-Salpeter equation with a kernel given by the functional derivative of $\Sigma_{\alpha\alpha'}(\vec{k}_{\parallel}, \omega | (L+d)-, (L+d)+)$ with respect to $d_{\beta\beta'}(\vec{k}_{\parallel}, \omega | (L+d)-, (L+d)+)$. If only the lowest-order term proportional to δ^2 is retained in $\Sigma_{\alpha\alpha'}$ [Eq. (27)], the corresponding Bethe-Salpeter equation corresponds to the ladder summation as illustrated in Fig. 2(c). Analytically we have

$$L_{ijkl}(\vec{k}_{||}, \vec{k}'_{||}, \omega) = \sum_{\alpha, \beta} d_{i\alpha}(\vec{k}_{||}, \omega | (L+d)-, (L+d)+) d_{k\beta}^*(\vec{k}_{||}, \omega | (L+d)-, (L+d)+) \\ \times \left[(2\pi)^2 \delta(\vec{k}_{||} + \vec{k}'_{||}) \delta_{j\alpha} \delta_{l\beta} + \delta^2 |\Lambda|^2 \int \frac{d^2 k''_{||}}{(2\pi)^2} g(|\vec{k}_{||} - \vec{k}''_{||}|) L_{\alpha j \beta l}(\vec{k}''_{||}, \vec{k}'_{||}, \omega) \right]. \quad (29)$$

For the intensity calculations we need $L_{ijkl}(\vec{k}_{||}, \vec{k}'_{||}, \omega | z_1, z'_1, z_2, z'_2)$ with general coordinates z_1, z'_1 lying anywhere outside and z_2, z'_2 anywhere inside the layered structure. This general case can be expressed in terms of $L_{ijkl}(\vec{k}_{||}, \vec{k}'_{||}, \omega)$ by

$$L_{ijkl}(\vec{k}_{||}, \vec{k}'_{||}, \omega | z_1, z'_1, z_2, z'_2) = (2\pi)^2 \delta(\vec{k}_{||} + \vec{k}'_{||}) d_{ij}(\vec{k}_{||}, \omega | z_1, z_2) d_{kl}^*(\vec{k}_{||}, \omega | z'_1, z'_2) \\ + \delta^2 |\Lambda|^2 \sum_{\alpha, \alpha'} d_{i\alpha}(\vec{k}_{||}, \omega | z_1, (L+d)+) d_{k\alpha'}^*(\vec{k}_{||}, \omega | z'_1, (L+d)+) \\ \times g(|\vec{k}_{||} + \vec{k}'_{||}|) d_{\alpha j}(-\vec{k}'_{||}, \omega | (L+d)-, z_2) d_{\alpha' l}^*(-\vec{k}'_{||}, \omega | (L+d)-, z'_2) \\ + \delta^4 |\Lambda|^4 \sum_{\substack{\alpha, \alpha' \\ \beta, \beta'}} d_{i\alpha}(\vec{k}_{||}, \omega | z_1, (L+d)+) d_{k\alpha'}^*(\vec{k}_{||}, \omega | z'_1, (L+d)+) \\ \times \int \frac{d^2 k''_{||}}{(2\pi)^2} g(|\vec{k}_{||} - \vec{k}''_{||}|) \int \frac{d^2 k'''_{||}}{(2\pi)^2} L_{\alpha \beta \alpha' \beta'}(\vec{k}''_{||}, \vec{k}'''_{||}, \omega) g(|\vec{k}'''_{||} - \vec{k}'_{||}|) \\ \times d_{\beta j}(-\vec{k}'_{||}, \omega | (L+d)-, z_2) d_{\beta' l}^*(-\vec{k}'_{||}, \omega | (L+d)-, z'_2). \quad (30)$$

The solution of the integral equation (29) was discussed in detail in Refs. 17 and 20 where the dominant contribution to $d_{ij}(\vec{k}_{||}, \omega | (L+d)-, (L+d)+)$ due to surface polariton alone was included. In Eq. (30) all those d_{ij} functions with z_1 and z'_1 as its coordinates must correspond to extended s - or p -polarized photons, whereas others correspond to SP. To solve Eq. (30) one can write in a general way

$$d_{ij}^{(0)}(\vec{k}_{||}, \omega | z, z') = d_{ij}^{(0s)}(\vec{k}_{||}, \omega | z, z') + d_{ij}^{(0p)}(\vec{k}_{||}, \omega | z, z'), \quad (31)$$

where the superscripts s and p denote s and p polarizations, respectively,

$$d_{ij}^{(0s)}(\vec{k}_{||}, \omega | z, z') = \frac{4\pi}{W_{\perp}(k_{||}, \omega)} [E_y^>(k_{||}, \omega | z) E_y^<(k_{||}, \omega | z') \Theta(z - z') \\ + E_y^<(k_{||}, \omega | z) E_y^>(k_{||}, \omega | z') \Theta(z' - z)] (\hat{k}_{||} \times \hat{z})_i (\hat{k}_{||} \times \hat{z})_j, \quad (32)$$

$$d_{ij}^{(0p)}(\vec{k}_{||}, \omega | z, z') = -\frac{4\pi}{W_{||}(k_{||}, \omega)} [e_i^<(\vec{k}_{||}, \omega | z) \Theta(z' - z) + e_i^>(-\vec{k}_{||}, \omega | z) \Theta(z - z')] \\ \times [e_j^>(\vec{k}_{||}, \omega | z') \Theta(z' - z) + e_j^<(-\vec{k}_{||}, \omega | z') \Theta(z - z')] + \Gamma(z) \delta(z - z') \delta_{iz} \delta_{jz}, \quad (33)$$

$$\vec{e}^<(\vec{k}_{||}, \omega | z) = E_x^<(k_{||}, \omega | z) \hat{k}_{||} + E_z^<(k_{||}, \omega | z) \hat{z}, \quad (34a)$$

$$\vec{e}^>(\vec{k}_{||}, \omega | z) = -E_x^>(k_{||}, \omega | z) \hat{k}_{||} + E_z^>(k_{||}, \omega | z) \hat{z}. \quad (34b)$$

The expressions for $\vec{E}^<>(k_{||}, \omega | z)$, $W_{\perp}(k_{||}, \omega)$, $W_{||}(k_{||}, \omega)$, and $\Gamma(z)$ are given in Ref. 11.

Using Eqs. (25)–(27) and only surface-polariton modes, we obtain

$$d_{ij}(\vec{k}_{||}, \omega | (L+d)-, (L+d)+) = \tilde{d}(k_{||}, \omega) e_i^<(\vec{k}_{||}, \omega | (L+d)-) e_j^>(\vec{k}_{||}, \omega | (L+d)+), \quad (35)$$

$$\tilde{d}(k_{||}, \omega) = \left[-\frac{W_{||}(k_{||}, \omega)}{4\pi} + \pi a^2 \delta^2 \Lambda^2 \int \frac{d^2 k'_{||}}{(2\pi)^2} \vec{e}^>(\vec{k}_{||}, \omega | (L+d)+) \cdot \vec{e}^<(\vec{k}'_{||}, \omega | (L+d)-) \right. \\ \left. \times \vec{e}^>(\vec{k}'_{||}, \omega | (L+d)+) \cdot \vec{e}^<(\vec{k}_{||}, \omega | (L+d)-) \frac{4\pi}{W_{||}(k'_{||}, \omega)} g(|\vec{k}_{||} - \vec{k}'_{||}|) \right]^{-1}. \quad (36)$$

The solution of the integral equation (29) can thus be written as^{17,20}

$$L_{ijkl}(\vec{k}_{||}, \vec{k}'_{||}, \omega) = e_i^<(\vec{k}_{||}, \omega | (L+d)-) e_k^{<*}(\vec{k}_{||}, \omega | (L+d)-) e_j^>(-\vec{k}'_{||}, \omega | (L+d)+) \\ \times e_l^>*(-\vec{k}'_{||}, \omega | (L+d)+) L(\vec{k}_{||}, \vec{k}'_{||}, \omega), \quad (37)$$

$$L(\vec{k}_{||}, \vec{k}'_{||}, \omega) = \sum_l L_l(k_{||}, k'_{||}, \omega) e^{i(\phi_k + \phi_{k'})}, \quad (38)$$

where $k_{||}$ and ϕ_k are the radial and angular components of $\vec{k}_{||}$, $l=0, 1, 2, -, -$, and

$$L_l(k_{||}, k'_{||}, \omega) = |\tilde{d}(k_{||}, \omega)|^2 \left[(2\pi/k_{||})\delta(k_{||} - k'_{||}) \right. \\ \left. + \pi a^2 \delta^2 |\Lambda|^2 |\tilde{d}(k'_{||}, \omega)|^2 \sum_{n, n'} (a_n^l a_{n'}^l)^{1/2} f_n^l(k_{||}) g_{n'}^l(k'_{||}) \{ [1 - P^l(\omega)]^{-1} \}_{nn'} \right]. \quad (39)$$

In Eq. (39)

$$P_{nn'}^l(\omega) = \pi a^2 \delta^2 |\Lambda|^2 (a_n^l a_{n'}^l)^{1/2} \int \frac{dk_{||}}{2\pi} k_{||} |\tilde{d}(k_{||}, \omega)|^2 g_n^l(k_{||}) f_{n'}^l(k_{||}), \quad (40)$$

where $f_n^l(k_{||})$, $g_n^l(k_{||})$, and a_n^l can be derived from

$$g(|\vec{k}_{||} - \vec{k}'_{||}|) |\vec{e}^>(\vec{k}_{||}, \omega | (L+d)+) \cdot \vec{e}^<(\vec{k}'_{||}, \omega | (L+d)-)|^2 = \pi a^2 \sum_l e^{i(\phi_k - \phi_{k'})} \sum_n a_n^l f_n^l(k_{||}) g_n^l(k'_{||}). \quad (41)$$

Explicit expressions of $f_n^0(k_{||})$, $g_n^0(k_{||})$, and a_n^0 are given in the Appendix of Ref. 17.

The integrals over $\vec{k}_{||}''$ and $\vec{k}_{||}'''$ in Eq. (30) can now be simplified. We first substitute Eqs. (37)–(39) for $L_{\alpha\beta\alpha'\beta'}(\vec{k}_{||}'', \vec{k}_{||}''', \omega)$ and Eq. (33) for d_{ij} in Eq. (30). [For s -photon emission use Eq. (32) instead of (33) for all d_{ij} with z_1, z_1' coordinates.] This gives terms depending only upon the relative angle between $\vec{k}'_{||}$ and $\vec{k}_{||}'''$ and between $\vec{k}_{||}$ and $\vec{k}_{||}''$. Thus the angular integration can be carried out by using the following partial wave expansion:

$$g(|\vec{k}_{||}''' + \vec{k}'_{||}|) |\vec{e}^>(\vec{k}_{||}''', \omega | (L+d)+) \cdot \vec{e}^<(\vec{k}'_{||}, \omega | (L+d)-)|^2 = \pi a^2 \sum_l e^{i(\phi_{k'''} + \phi_{k'})} \sum_n a_n^l f_n^l(k_{||}''') \tilde{g}_n^l(k'_{||}), \quad (42)$$

$$g(|\vec{k}_{||} - \vec{k}_{||}''|) |\vec{e}^>(-\vec{k}_{||}, \omega | (L+d)+) \cdot \vec{e}^<(\vec{k}_{||}'', \omega | (L+d)-)|^2 = \pi a^2 \sum_l e^{i(\phi_k - \phi_{k''})} \sum_n a_n^l \tilde{f}_n^l(k_{||}) g_n^l(k_{||}''), \quad (43)$$

where the functions $\tilde{f}_n^l(k_{||})$ and $\tilde{g}_n^l(k_{||})$ are listed in the Appendix. The integrals over radial parts can be carried out by using the following identity¹⁷

$$\pi a^2 \delta^2 |\Lambda|^2 \int \frac{dk_{||}''}{2\pi} k_{||}'' \int \frac{dk_{||}'''}{2\pi} k_{||}''' (a_n^l a_{n'}^l)^{1/2} g_n^l(k_{||}'') f_{n'}^l(k_{||}''') L_l(k_{||}'', k_{||}''', \omega) = \{ [1 - P^l(\omega)]^{-1} \}_{nn'} - \delta_{nn'}. \quad (44)$$

Thus Eq. (30) can be simplified by using Eqs. (42)–(44). Substituting the result in Eq. (11) and using the expressions of Ref. 11 for $\vec{E}^>(\vec{k}_{||}, \omega | z)$, we have after some minor simplifications for p -polarized emission as follows:

$$\frac{dQ(\omega)}{d\Omega} = \frac{e^2}{\pi \hbar c} \left[\frac{eV}{\hbar \omega} - 1 \right] \frac{\omega^4}{c^4} \left| \frac{\cos\theta}{\sin\theta} \frac{1}{W_{||}(k_{||}, \omega)} \right|^2 \int \frac{dQ_{||}}{2\pi} \frac{Q_{||}}{(1 + Q_{||}^2 \epsilon_0^2)^{3/2}} \left| \int_0^{L+d} dz E_z^<(Q_{||}, \omega | z) \right|^2 \\ \times \left[\frac{2\pi}{Q_{||}} \delta(k_{||} - Q_{||}) + \pi a^2 \delta^2 |\Lambda|^2 \sum_{n, n'} (a_n^0 a_{n'}^0)^{1/2} \tilde{f}_n^0(k_{||}) \{ [1 - P^0(\omega)]^{-1} \}_{nn'} \tilde{g}_{n'}^0(Q_{||}) |\tilde{d}(Q_{||}, \omega)|^2 \right]. \quad (45)$$

Note that $k_{||} = (\omega/c)\sin\theta$ and in writing Eq. (45) only the dominant contribution due to $l=0$ term in the summation is retained.^{17,20} A similar expression holds for s -photon emission. It is obtained by omitting the first term in the second set of large parentheses in Eq. (45), by using the expression for $\tilde{f}_n^0(k_{||})$ for s photons from the Appendix and by replacing the factor $|\cos\theta/\sin\theta| [1/W_{||}(k_{||}, \omega)]^2$ by $|\cos\theta/W_{\perp}(k_{||}, \omega)|^2$.

In Eq. (45) the first term in the second set of large parentheses corresponds to the direct p -photon emission, i.e., from the smooth surface. The second term proportional to δ^2 is due to the rough surface. The lowest-order perturbation results of Ref. 11 can be obtained by substituting $P^0(\omega)=0$ in Eq. (45). Thus the nonperturbative

factor $[1 - P^0(\omega)]^{-1}$ in Eq. (45) gives contribution due to multiple scattering of SP modes at the rough surface. Our numerical calculations show (see next section) that this term is, in general, not small for realistic roughness parameters.

III. RESULTS AND DISCUSSION

We now give numerical results for the photoemission intensities calculated from Eq. (45). The main contribution comes from the roughness-dependent second term in the second set of large parentheses of Eq. (45). The first term corresponding to the direct coupling of the tunneling electrons to the photons is usually very small. The following parameters for the tunnel junctions are chosen: thick-

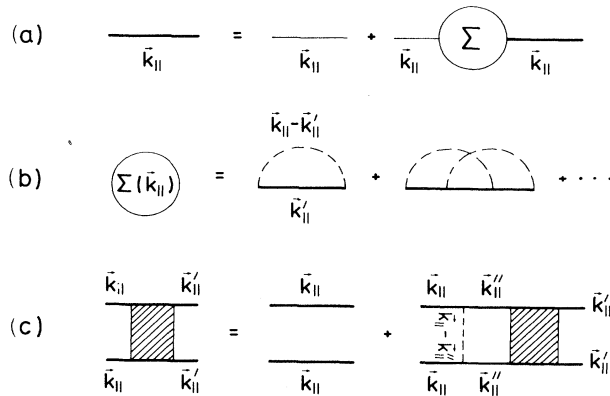
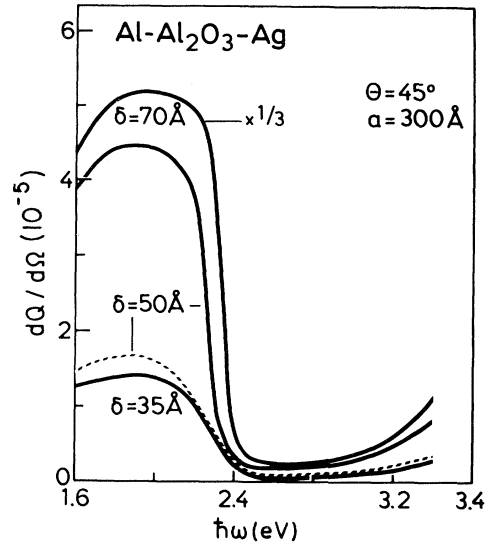


FIG. 2. (a) Dyson equation for the averaged one-photon propagator $d_{ij}(\bar{k}_{||}, \omega | z, z')$. (b) Self-energy diagrams; the dashed line denotes the interaction $\delta^2 \Lambda^2 g(|\bar{k}_{||} - \bar{k}'_{||}|)$ due to roughness. (c) Bethe-Salpeter equation for the averaged two-photon propagator.

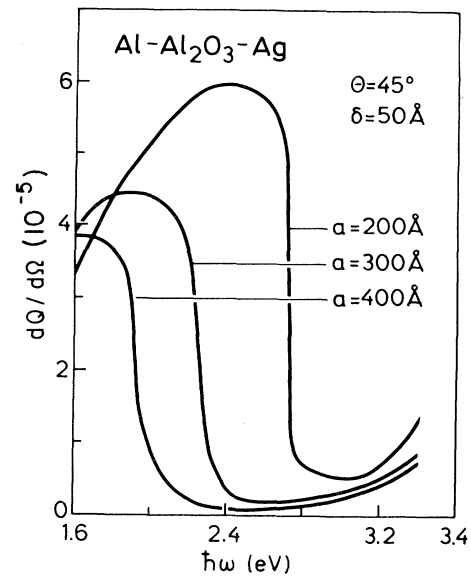
ness of the oxide layer $d = 30 \text{ \AA}$, thickness of the metal (Ag or Au) film $L = 200 \text{ \AA}$, dielectric constant of oxide layer $\epsilon_2 = 3$. The dielectric function ϵ_1 of the metal (Ag or Au) is taken from the experiments of Johnson and Christy²² and ϵ_3 of Al from Ref. 23. In all these calculations $\xi_0 = 100 \text{ \AA}$.

Figures 3(a) and 3(b) show total (*s*- and *p*-) photoemission intensities from Al-Al₂O₃-Ag as a function of the emitted photon frequency ω . The applied voltage is 4 V and $\theta = 45^\circ$. Figure 3(a) has been calculated for $a = 300 \text{ \AA}$ and $\delta = 35, 50, \text{ and } 70 \text{ \AA}$. The dashed curve is the result of perturbation theory. For frequencies $\omega \leq 2.3 \text{ eV}$, the photon yield $10^5(dQ/d\Omega)$ lies between 1 and 15 and then falls rapidly to values ~ 0.2 . Figure 3(b) is for $\delta = 50 \text{ \AA}$ and $a = 200, 300, \text{ and } 400 \text{ \AA}$. In each curve the intensity drops again rapidly at a frequency which depends on the value of a .

These results can be understood by considering the contributions from different SP modes. For MOM layered structure with smooth surfaces, the dispersion curves for the surface polaritons are obtained from Eq. (33), i.e., by $W_{||}(k_{||}, \omega) = 0$. There are three solutions: (i) the slow or junction mode in which the fields are concentrated in the junction, (ii) the fast Ag-vacuum interface mode, and (iii) the fast Al-oxide interface mode (for more discussions see Refs. 6 and 24). In the visible frequency range the phase velocity of the fast modes is quite close to the velocity of light in vacuum, whereas that of the slow mode is much smaller. With the above parameters for Al-Al₂O₃-Ag, the upper cut-off frequency for the slow mode is $\sim 3.2 \text{ eV}$ and for the fast Ag-vacuum interface mode $\sim 3.5 \text{ eV}$. Our numerical calculations [see Eqs. (40) and (45)] include contributions from all these modes. For lower frequencies the dominant contribution comes from the slow SP mode because of a large phase space available for its scattering at the rough surface. For higher frequencies the wave vector $k_{||}$ of the slow mode becomes large and the exponential factor $\exp(-k_{||}^2 a^2/2)$ in the Gaussian distribution reduces its contribution rapidly. This explains why in Fig. 3(b) the drop in intensities occurs at lower frequencies



(a)



(b)

FIG. 3. Roughness-induced emission spectrum from Al-Al₂O₃-Ag tunnel junction at an angle $\theta = 45^\circ$ with the normal, and an applied voltage of 4 V and different values for δ and a . Curve for $\delta = 70 \text{ \AA}$ is multiplied by a factor $\frac{1}{3}$. Dashed curve in (a) corresponds to lowest-order perturbation theory.

for larger values of a . For still higher frequencies the contribution to emission comes from the fast Ag-vacuum interface mode. The small increase in the intensities with frequency (less than or equal to 3.5 eV) is due to the increase in phase space available for the roughness induced scattering of fast mode.

The comparison of the dashed and the solid lines for $\delta = 50 \text{ \AA}$ in Fig. 3(a) also shows that multiple scattering of surface polaritons leads to a substantial increase in the intensity of the emitted light over a broad-frequency region.

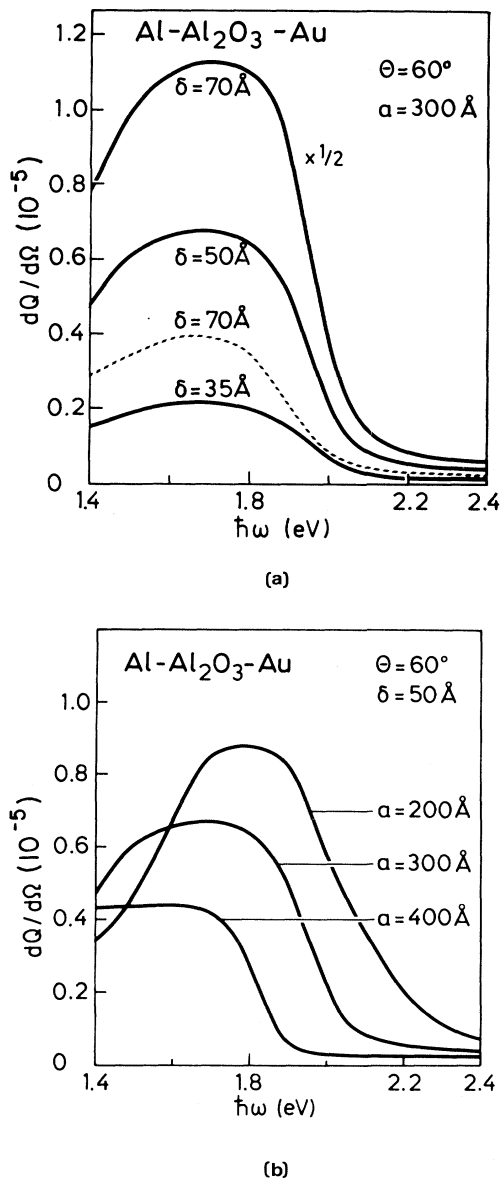


FIG. 4. Same as in Fig. 3 for Al-Al₂O₃-Au tunnel junction and $\theta=60^\circ$. Scale factor for the curve with $\delta=70 \text{ \AA}$ is $\frac{1}{2}$.

This implies that our nonperturbative treatment of roughness is absolutely necessary for the used parameters in order to obtain quantitative results.

Figures 4(a) and 4(b) show similar results for Al-Al₂O₃-Au. Following Ref. 4, we have used bias voltage to the junction $=2.7 \text{ V}$ and $\theta=60^\circ$. Figure 4(a) is for $a=300 \text{ \AA}$ and $\delta=35, 50, \text{ and } 70 \text{ \AA}$. Figure 4(b) is for $\delta=50 \text{ \AA}$ and $a=200, 300, \text{ and } 400 \text{ \AA}$. The photon yield $10^5(dQ/d\Omega)$ lies between 0.2 and 2.5 for $\hbar\omega \leq 2 \text{ eV}$ in agreement with experiments of Ref. 4. The main contribution in this frequency range is due to the multiple scattering of the slow SP mode. The fast SP modes contribute very little in the high-frequency range because of large damping due to the large imaginary part of the dielectric function ϵ_1 of gold. For the roughness parameters, the calculated emission intensity shows a broad peak

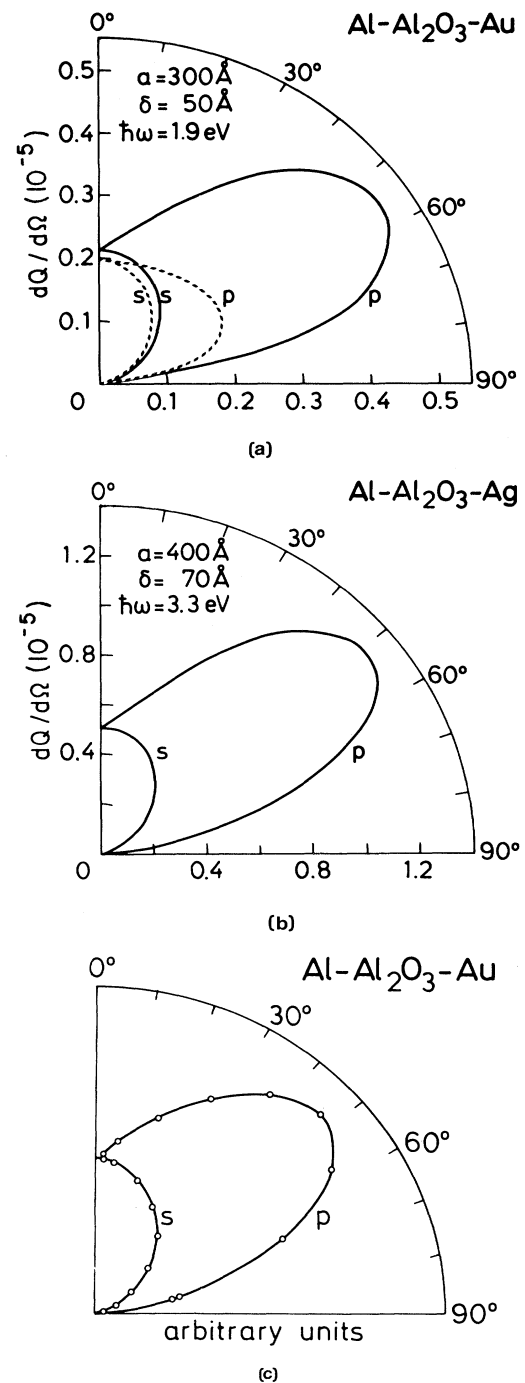


FIG. 5. Angular distribution of *s*- and *p*-polarized light (solid lines) where the angle θ is measured with respect to the normal to the surface. (a) For Al-Al₂O₃-Au and $a=300 \text{ \AA}$, $\delta=50 \text{ \AA}$, $\hbar\omega=1.9 \text{ eV}$, and a bias voltage of 2.7 V . Dashed curves are the result of first-order perturbation; (b) for Al-Al₂O₃-Ag and $a=400 \text{ \AA}$, $\delta=70 \text{ \AA}$, $\hbar\omega=3.3 \text{ eV}$, and a bias voltage of 4 V ; (c) experimental results of Ref. 4 for Al-Al₂O₃-Au tunnel junction.

around $1.8\text{--}1.9 \text{ eV}$. This is also in agreement with experiments. Comparison of the dashed and solid lines for $\delta=70 \text{ \AA}$ in Fig. 4(a) shows again the important role of multiple scattering: The photon yield increases by this ef-

fect over a broad region around the maximum by about a factor of 6.

The angular distribution of the emitted light is plotted in Figs. 5(a) and 5(b). Figure 5(a) is for Al-Al₂O₃-Au with $\delta=50$ Å, $a=300$ Å, $\hbar\omega=1.9$ eV and bias voltage = 2.7 V. Figure 5(b) is for Al-Al₂O₃-Ag with $\delta=70$ Å, $a=400$ Å, $\hbar\omega=3.3$ eV, and bias voltage = 4 V. The calculated intensities have both *s* and *p* components [solid lines in Figs. 5(a) and 5(b)]. By symmetry the intensities of *s* and *p* components are equal along the normal to the surface. The intensity of the *s* component smoothly decreases as one goes away from the normal and then becomes zero along the surface. However, the *p* component shows a lobe structure around an angle of 50°–60° off the normal and then falls to zero along the surface. The calculated curves for Al-Al₂O₃-Au [solid curves in Fig. 5(a)] agree well with the experimental curves of Ref. 4 which are reproduced in Fig. 5(c). The dashed curves in Fig. 5(a) are the results of first-order perturbation theory. The *s* component is nearly unchanged. However, the perturbational *p* component shows only a weak maximum off the normal which is also in disagreement with experiment. The observed pronounced maximum is therefore due to the multiple scattering of SP.

The experiments of Ref. 2 show that the emission intensity first increases with the roughness amplitude δ and then gets saturated. In our theory the roughness amplitude enters in two ways. (a) The coupling of SP with photon increases with δ and hence the photoemission intensity. The intensity, however, is not proportional to δ^2 as in the perturbation results of Ref. 11 but depends in a different way through the presence of δ^2 also in the matrix elements $P_{nn}^0(\omega)$ [see Eq. (40)]. (b) The self-energy of SP increases with increasing δ [see Eq. (27)]. The increase in the imaginary part of the self-energy decreases the life time of SP and hence makes the coupling with photons weaker. The result should be a decrease in the emission intensity. Figures 3(a) and 3(b) show an increase in the intensity as δ varies from 35 to 70 Å. In this range of δ values the width of SP increases, but this increase is not sufficient to saturate the intensity. The saturation may start occurring for larger values of δ which, however, cannot be treated adequately within our approximations: Higher-order terms in the self-energy (e.g., second diagram in Fig. 2(b)) as well as the corresponding contributions to the kernel of the Bethe-Salpeter equation [leading to crossed diagrams, in addition to the ladder diagrams in Fig. 2(c)] must then be included. However, for the roughness parameters reported in this paper, we have checked that the contribution to the self-energy from the second diagram in Fig. 2(b) is small compared to that from the first diagram. Contributions due to crossed diagrams in the Bethe-Salpeter equation can therefore also be neglected.

ACKNOWLEDGMENTS

The authors thank Professor Alexei A. Maradudin for suggesting this problem and for many stimulating discussions.

APPENDIX

In this appendix we give expressions for $\tilde{g}_n^0(Q_{||})$ and $\tilde{f}_n^0(k_{||})$ derived from Eqs. (42) and (44), respectively. The derivation is similar to that given in the Appendix of Ref. 17 for $g_n^l(k_{||})$ and $f_n^l(k_{||})$. We thus omit any details here and give the final expressions

$$\tilde{g}_1^0(Q_{||}) = |1/\epsilon_1|^2 e^{-2\nu_0(L+d)} e^{-Q_{||}^2 a^2/4}, \quad (\text{A1})$$

$$\tilde{g}_2^0(Q_{||}) = (\nu_0 a / |\epsilon_1|) e^{-2\nu_0(L+d)} e^{-Q_{||}^2 a^2/4}, \quad (\text{A2})$$

$$\tilde{g}_3^0(Q_{||}) = (\nu_0/Q_{||})^2 e^{-2\nu_0(L+d)} e^{-Q_{||}^2 a^2/4}, \quad (\text{A3})$$

$$\tilde{g}_{3p+q}^0(Q_{||}) = \tilde{g}_q^0(Q_{||}) (Q_{||} a / \sqrt{2})^{2p}, \quad (\text{A4})$$

$q=1,2,3$, and $p=1,2,-,-,-$. Also $\nu_0 = (Q_{||}^2 - \omega^2/c^2)^{1/2}$, where $Q_{||} > \omega/c$ for the SP mode. As in Ref. 17 we have neglected small imaginary parts of ϵ_1 and ϵ_3 for simplicity.

There are two different expressions for $\tilde{f}_n^0(k_{||})$ corresponding to *p*- and *s*-polarized emission. For *p* photons, using Eq. (34) for $\vec{e}^<(-\vec{k}_{||}, \omega | (L+d)+)$, we find from Eq. (43)

$$\tilde{f}_1^0(k_{||}) = |n_z(k_{||}, \omega)|^2 e^{-k_{||}^2 a^2/4}, \quad (\text{A5})$$

$$\tilde{f}_2^0(k_{||}) = ik_0 a n_z(k_{||}, \omega) n_x(k_{||}, \omega) e^{-k_{||}^2 a^2/4}, \quad (\text{A6})$$

$$\tilde{f}_3^0(k_{||}) = |(k_0/k_{||}) n_x(k_{||}, \omega)|^2 e^{-k_{||}^2 a^2/4}, \quad (\text{A7})$$

$k_{||} = (\omega/c)\sin\theta$, $k_0 = (\omega/c)\cos\theta$, and ω is the frequency of the emitted photon. $n_x(k_{||}, \omega)$ and $n_z(k_{||}, \omega)$ are defined by Eqs. (2.34b) and (2.34c) of Ref. 11, respectively. For $n > 3$, $\tilde{f}_n^0(k_{||})$ are given by a relation similar to (A4). However, because of the factor $(k_{||} a / \sqrt{2})^{2p}$ which is very small for photon frequencies of interest, the $\tilde{f}_n^0(k_{||})$'s are very small for $n > 3$ and are neglected.

For *s* photons, $\vec{e}^<(-\vec{k}_{||}, \omega | (L+d)+)$ in Eq. (43) is to be replaced by $E_y^<(k_{||}, \omega | (L+d)+)(\hat{k}_{||} \times \hat{z})$ and we find

$$\tilde{f}_1^0(k_{||}) = 0, \quad (\text{A8})$$

$$\tilde{f}_2^0(k_{||}) = 0, \quad (\text{A9})$$

$$\tilde{f}_3^0(k_{||}) = |n_y(k_{||}, \omega)|^2 e^{-k_{||}^2 a^2/4}, \quad (\text{A10})$$

where $n_y(k_{||}, \omega)$ is defined by Eq. (2.34d) of Ref. (11) and $k_{||} = (\omega/c)\sin\theta$. The $\tilde{f}_n^0(k_{||})$'s are again neglected for $n > 3$.

*Present address: Department of Physics, City College, CUNY, New York, NY 10031.

¹J. Lambe and S. L. McCarthy, Phys. Rev. Lett. **37**, 923 (1976).

²S. L. McCarthy and J. Lambe, Appl. Phys. Lett. **30**, 427

(1977); **33**, 858 (1978).

³P. K. Hansma and H. P. Broida, Appl. Phys. Lett. **32**, 545 (1978).

⁴A. Adams, J. C. Wyss, and P. K. Hansma, Phys. Rev. Lett. **42**,

- 912 (1979).
- ⁵R. K. Jain, S. Wagner, and D. H. Olson, *Appl. Phys. Lett.* **32**, 62 (1978).
- ⁶J. Kirtley, T. N. Theis, and J. C. Tsang, *Phys. Rev. B* **24**, 5650 (1981).
- ⁷N. Kroo, Zs. Szentirmay, and J. Felszerfalvi, *Phys. Lett.* **81A**, 399 (1981).
- ⁸D. G. Walmsley, H. F. Quinn, and P. Dawson, *Phys. Rev. Lett.* **49**, 892 (1982).
- ⁹K. Parvin and W. Parker, *Solid State Commun.* **37**, 629 (1981).
- ¹⁰L. C. Davis, *Phys. Rev. B* **16**, 2482 (1977).
- ¹¹B. Laks and D. L. Mills, *Phys. Rev. B* **20**, 4962 (1979).
- ¹²B. Laks and D. L. Mills, *Phys. Rev. B* **21**, 5175 (1980).
- ¹³B. Laks and D. L. Mills, *Phys. Rev. B* **22**, 5723 (1980).
- ¹⁴D. L. Mills, M. Weber, and B. Laks, in *Tunneling Spectroscopy: Capabilities, Applications, and New Techniques*, edited by P. K. Hansma (Plenum, New York, 1982), Chap. 5.
- ¹⁵D. Hone, B. Muhlschlegel, and D. J. Scalapino, *Appl. Phys. Lett.* **33**, 203 (1978); R. W. Rendell, D. J. Scalapino, and B. Muhlschlegel, *Phys. Rev. Lett.* **41**, 1746 (1978).
- ¹⁶R. W. Rendell and D. J. Scalapino, *Phys. Rev. B* **24**, 3276 (1981).
- ¹⁷K. Arya and R. Zeyher, *Phys. Rev. B* **28**, 4090 (1983).
- ¹⁸G. Baym and L. P. Kadanoff, *Phys. Rev.* **124**, 287 (1961).
- ¹⁹G. Baym, *Phys. Rev.* **127**, 1391 (1962).
- ²⁰K. Arya, R. Zeyher, and A. A. Maradudin, *Solid State Commun.* **42**, 461 (1982).
- ²¹A. A. Maradudin and W. Zierau, *Phys. Rev. B* **14**, 484 (1976).
- ²²P. B. Johnson and R. W. Christie, *Phys. Rev. B* **6**, 4370 (1972).
- ²³J. C. Powell, *Phys. Rev.* **60**, 78 (1970).
- ²⁴E. N. Economou, *Phys. Rev.* **182**, 539 (1969).